JOURNAL OF MATERIALS SCIENCE 27 (1992) 1297–1301

Supercritical drying of SiO_2–TiO_2 sol-pillared clays

K. TAKAHAMA, M. YOKOYAMA, S. HIRAO
Central Research Laboratory, Matsushita Electric Works Ltd, 1048 Kadoma, Osaka 571, Japan
S. YAMANAKA, M. HATTORI
Department of Applied Chemistry, Faculty of Engineering, Hiroshima University, Higashi-Hiroshima 724, Japan

The interlayers of montmorillonite clay were pillared with silica–titania sol particles by ion exchange in aqueous solutions. The water in the pillared clay was substituted with ethanol which was in turn extracted with CO_2 under supercritical conditions. This drying procedure avoids the formation of liquid–vapour interfaces which give rise to shrinkage of the swelled pillared structure. Highly porous structures with well developed card-house structures resulted. The pore structure was investigated and compared with that of samples prepared by conventional air-drying procedures.

1. Introduction

Montmorillonite is the commonest clay mineral of the smectite group, the structure of which is composed of stacked two-dimensional aluminosilicate layers. The aluminium cations of the silicate layers are partially substituted by lower valent cations such as Mg^{2+} and Fe^{2+}, and the resulting net negative charges are balanced with hydrated exchangeable cations located between the silicate layers. It is well known that various kinds of polar organic molecules are intercalated into the interlayer spaces of montmorillonite [1]. Most of the intercalated layers, however, readily collapse if these are heated or evacuated, and non-polar molecules which cannot have strong interactions with the interlayer cations are not allowed to intercalate into the interlayer space. In order to make the interlayer spaces more open and more easily accessible to non-polar as well as polar molecules, the silicate layers have been pillared with ceramic oxides.

Pillared clays are prepared by exchanging the interlayer cations of montmorillonite with voluminous hydroxy–metal cations such as $[Al_{13}O_4(OH)_{24}]^{7+}$ [2, 3] and $[Zr_4(OH)_{14}]^{2+}$ [4] in aqueous media [5, 6], which are then converted into the corresponding oxide pillars between the silicate layers by calcination. Yamanaka *et al.* [7–9] have reported that oxide sol particles such as TiO_2 and SiO_2–TiO_2 can also be directly intercalated by ion exchange, as long as the particles are positively charged. The pore structures formed between the silicate layers are controllable over a wide range from micro- to mesopore regions by pillaring with oxides with controlled particle sizes. The chemical activity or affinity of the pores may also be varied by using a variety of oxide pillars.

The ion exchange of the interlayer cations of montmorillonite with precursor cations for pillars is usually carried out in aqueous media, and the samples separated after the ion exchange are extremely swelled with water. The swelled sample experiences remarkable shrinkage during drying, as in the case of the drying of aqueous gels formed by a solution–sol–gel route [10, 11]. The shrinkage of the gel is caused by the large liquid–vapour interfacial (capillary) forces, which act to disrupt the delicate microporous gel structure during an evaporative drying procedure [2, 11]. The porous structures of the swelled pillared clays must also be very different before and after the shrinkage on drying.

Recently a new drying technique, supercritical drying, has been developed in which the solvent in the gel pores is substituted by a fluid with a relatively low critical temperature, and the fluid is extracted supercritically avoiding the formation of liquid–vapour interfaces [12]. This technique has been successfully applied to the preparation of highly porous and translucent silica aerogels from alcogel by using a supercritical CO_2 fluid [13].

In this study, a similar supercritical drying technique is applied to the drying of SiO_2–TiO_2 sol-pillared clays, and the resulting pore structure has been investigated in comparison with that of the sample prepared by conventional air-drying procedures.

2. Experimental procedure

2.1. Preparation of pillared clays

The clay used in this study was Na-montmorillonite (Kunipia F) supplied from Kunimine Industrial Company, Japan, which is the same clay as used in previous studies [7, 9, 14]. Its structural formula was determined to be $(Na_{0.35}K_{0.01}Ca_{0.02})(Si_{3.89}Al_{0.11})(Al_{1.60}Mg_{0.32}Fe_{0.08})O_{10}(OH)_2\ nH_2O$, and its cation exchange capacity was measured to be 100 meq per 100 g.

0022–2461

The montmorillonite was pillared with silica–titania sol particles by the following ion-exchange procedures. The titania sol solution was prepared by the hydrolysis of titanium tetraisopropoxide, $Ti(OC_3H_7)_4$ with 1 N HCl solution in a molar ratio of $HCl/Ti(OC_3H_7)_4 = 4$; the resulting precipitate was peptized by further stirring at room temperature. The silica sol solution was prepared by the hydrolysis of silicon tetraethoxide, $Si(OC_2H_5)_4$ by adding 1 N HCl solution and ethanol in a ratio of $Si(OC_2H_5)_4$/1 N HCl/C_2H_5OH = 41.6 g/10 ml/12 ml. The two sol solutions were mixed in a ratio of $TiO_2/SiO_2 = 1/10$. The silica sol particles with negative charges were changed into positively charged sol by the addition of the titania sol solution, and became exchangeable with the interlayer sodium cations of montmorillonite [8, 9, 14]. The exchange was performed by mixing 1% montmorillonite suspension in water with the silica–titania mixed-sol solution in such a way that the molar ratio SiO_2/TiO_2/CEC = 4/0.4/1, where CEC denotes the molar equivalent of the cation exchange capacity of montmorillonite. After the mixture was allowed to stand for 1.5 h under stirring at 60 °C, the pillared product was separated and washed with water several times by centrifugation.

2.2. Supercritical drying

The washed and centrifuged products were rinsed with ethanol three times by centrifugation in order to replace the water in the product with the ethanol, which was then extracted with supercritical fluid of CO_2 under a pressure of 120 atm at 40 °C. The CO_2 was vented for 5 h. For comparison, a separate sample of SiO_2–TiO_2 pillared clay was similarly prepared and air-dried at 60 °C. The samples thus prepared by the two different drying procedures were calcined at 500 °C for 3 h in air, and supplied for the following analyses.

2.3. Analyses

X-ray powder diffraction (XRD) patterns were measured by using graphite monochromatized Ni$K\alpha$ radiation. Chemical analyses of the pillared clay were carried out by the atomic absorption method described elsewhere [9]. An AUTOSORB 6 from Quantachrome Corporation was used to measure N_2 adsorption–desorption isotherms at liquid-nitrogen temperature. An AUTOPORE 9200 from Micrometrics Instrument Corporation was used for mercury penetration porosimetry. Scanning electron micrographs (SEM) were taken on the samples sputter-coated with 20-nm-thick Pt–Pd (90–10%). High-resolution electron microscope (HREM) images were taken with a Jeol JEM-200C microscope on the powder sample deposited onto a Cu microgrid.

3. Results

3.1. Chemical analysis

The chemical analysis data of the air-dried sample are shown in Table I, together with those of the initial Na-montmorillonite used. Both samples were analysed after calcination at 800 °C. The composition of interlayer pillars was estimated by assuming that the composition of the silicate layers of montmorillonite was unchanged by the pillaring. The total silica content found in the pillared clay was divided and assigned to the silicate layer and interlayer pillar origins as shown in Table I. The composition of the pillar is very similar to that of the sol solution used for the ion exchange, and about 90% of the sol used is taken up by montmorillonite.

TABLE I Chemical analysis data of the pillared clay in comparison with those of the initial Na-montmorillonite calcined at 800 °C

	Na-montmorillonite	Pillared clay
SiO_2	66.3	74.1
Al_2O_3	24.5	14.3
MgO	2.01	1.17
Na_2O	3.03	–
TiO_2	–	5.99
Total	95.84%	95.56%
Composition in atomic ratios on $O_{10}(OH)_2$ anion basis:		
Silicate layer		
Si	3.89	3.89
$Al^{(IV)}$	0.11	0.11
$Al^{(VI)}$	1.60	1.60
Mg	0.32	0.32
Interlayer composition		
Na	0.35	–
Si	–	3.63
Ti	–	0.46

3.2. X-ray diffraction study

The XRD patterns of the samples prepared by the two different drying procedures are compared in Fig. 1. In the preparation of the air-dried sample for XRD measurement, the wet pillared sample was spread on a glass slide before drying so as to attain a preferred orientation, and then calcined at 500 °C on the slide.

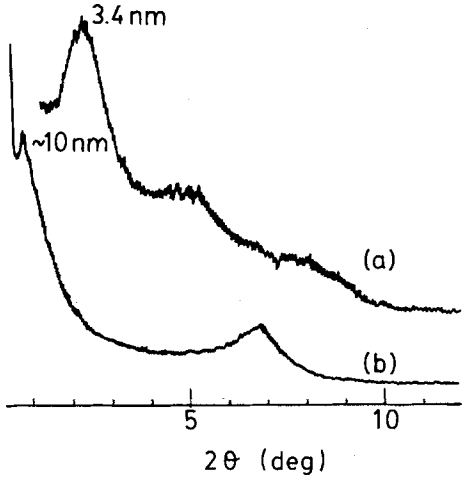

Figure 1 XRD patterns of the two pillared clays calcined at 500 °C. (a) Air-dried, (b) supercritically dried.

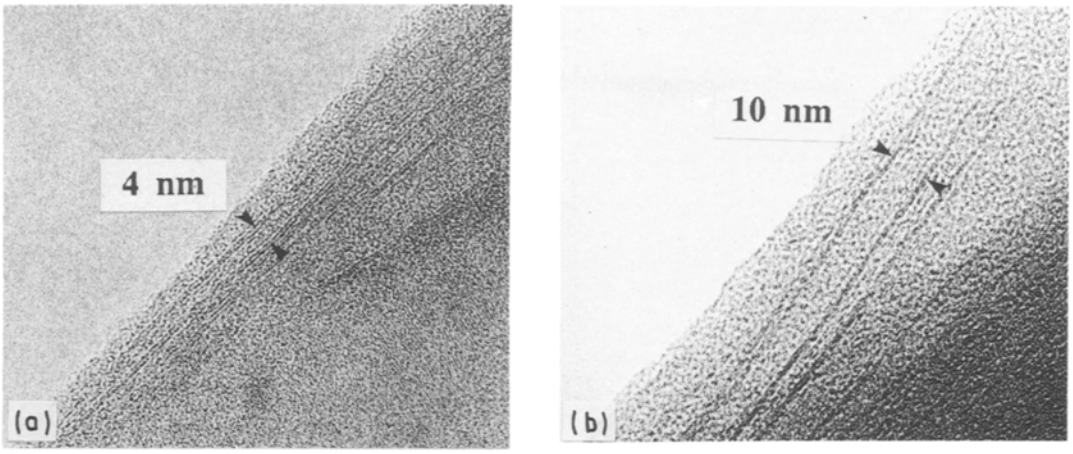

Figure 2 HREM micrographs of the two pillared clays. (a) Air-dried, (b) supercritically dried.

The XRD pattern clearly showed three integral reflection peaks for a basal spacing of 3.4 nm. For the XRD measurement of the supercritically dried (SCD) sample, the dried and calcined sample was filled in a cavity of a glass slide. The latter sample was therefore, more randomly oriented, and showed only a weak shoulder reflection, corresponding to a basal spacing of about 10 nm and a broad reflection peak for a smaller basal spacing of 1.2 nm. Since the thickness of the silicate layer itself is 0.96 nm, the appearance of the small spacing can be explained in terms of the occurrence of a partial collapse in the pillared structure during the drying. The two samples compared in Fig. 1 do not have similar orientation and thus cannot be compared in a simple manner. However, it appears that the SCD sample has a much larger basal spacing than the air-dried sample.

HREM photographs were taken of the powder samples deposited on the microgrid of an electron microscope. Fig. 2 shows typical HREM images measured on the edges of the powder samples. Silicate layers running in parallel along the edge were observed in the images, where the silicate layers of the pillared clays might be curved in such a way that the electron beam of incidence was parallel to the silicate sheets. As marked in the micrographs, the separations of the silicate layers observed almost corresponds to the basal spacings obtained by the above XRD study. The SCD sample has a tendency to have larger basal spacings than the air-dried sample.

3.3. Nitrogen adsorption

The nitrogen adsorption–desorption isotherms for the two samples calcined at 500 °C are compared in Fig. 3. The adsorption isotherm of the air-dried sample is characterized as type I or type II, with a restricted number of nitrogen adsorption layers. This indicates that most of the pores formed in the air-dried sample are in a micro- to small mesopore region. The SCD sample also has a similar adsorption isotherm in the lower pressure region, but the isotherm rises steeply in the higher pressure region due to a capillary condensation. This suggests that the SCD sample contains a wide range of meso- as well as micropores. Another

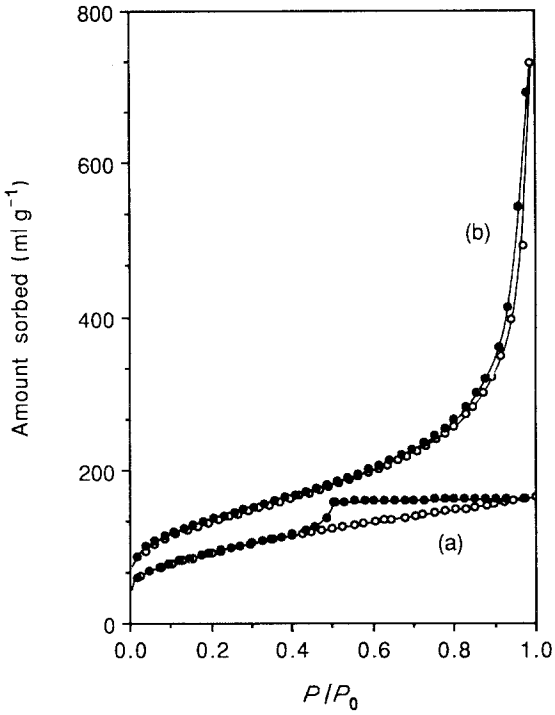

Figure 3 Nitrogen adsorption–desorption isotherms for the two pillared clays calcined at 500 °C. (a) Air-dried, (b) supercritically dried; ○, adsorption; ●, desorption.

characteristic feature of the SCD sample is to show little hysteresis for desorption. The pores in the SCD sample must be very open and have a small number of ink-bottle type necks. The BET surface areas for nitrogen were determined to be 325 and 459 $m^2 g^{-1}$ for the air-dried and the SCD samples, respectively. The pore-size distributions of the two samples were calculated on the basis of the respective adsorption branches and the procedures developed by Barrett *et al.* [15], which are shown in Fig. 4. The curves indicate that the SCD sample has a broader pore-size distribution over a wide pore-size range, although the two samples compared have similar distributions in a pore-size range smaller than 2 nm in radius.

3.4. Mercury porosimetry

Pore-size distributions in the region larger than about 10 nm in diameter were analysed by mercury intrusion

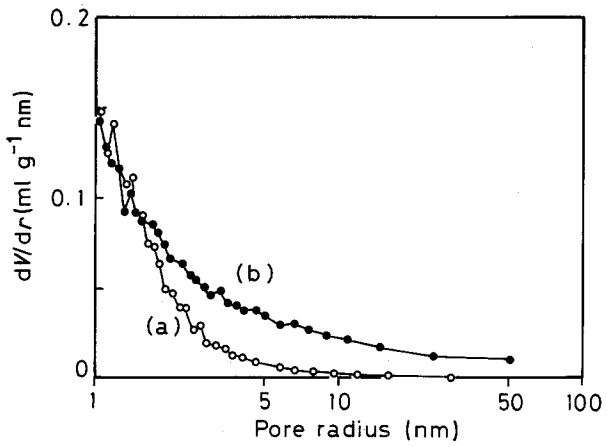

Figure 4 Pore-size distribution of the pillared clays calculated on the basis of the adsorption isotherms shown in Fig. 3. (a) Air-dried, (b) supercritically dried.

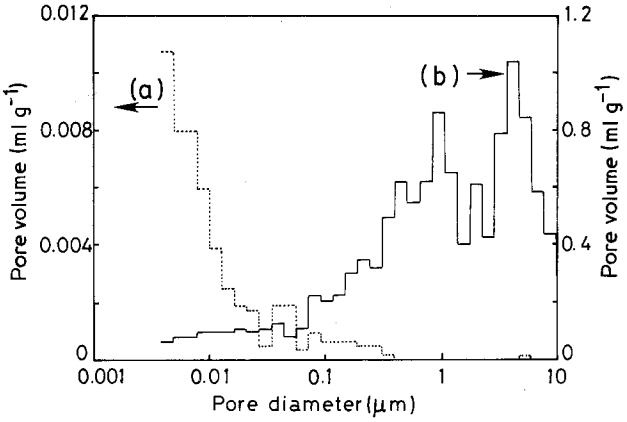

Figure 5 Pore-volume distributions of the two pillared clays measured by a mercury porosimeter. (a) Air-dried (dotted line), (b) supercritically dried (solid line).

TABLE II Pore volumes (porosities) measured by nitrogen adsorption and the mercury porosimetry

Drying procedure	Nitrogen adsorption ($ml\,g^{-1}$)	Mercury porosimetry ($ml\,g^{-1}$)
Supercritical drying	1.06	9.82
Air drying	0.19	0.098

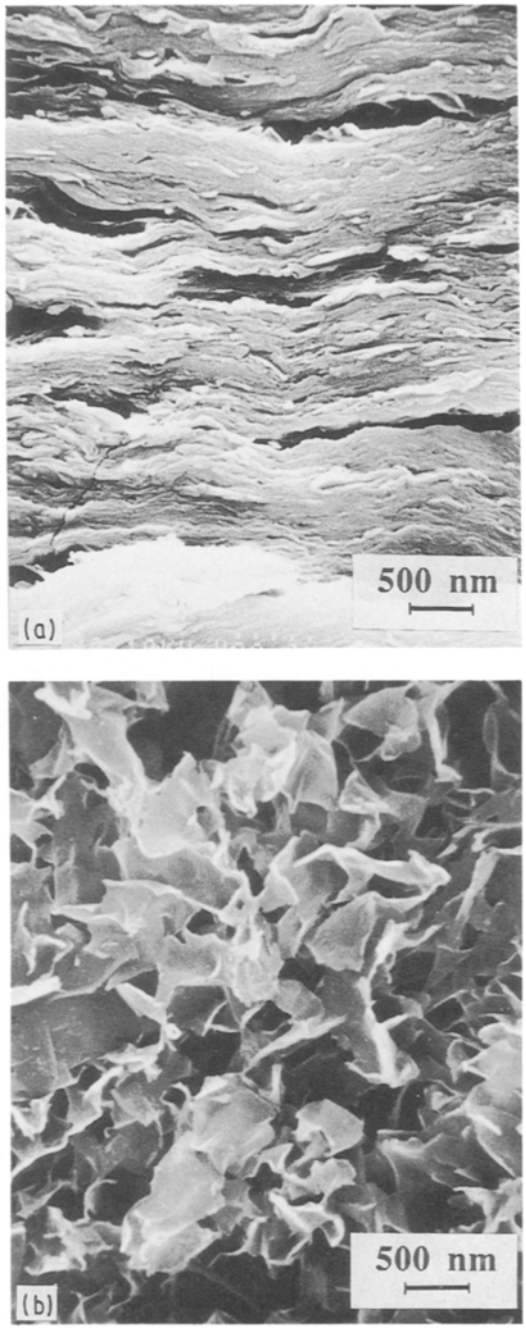

Figure 6 SEM photographs of the two pillared clays. (a) Air-dried, (b) supercritically dried.

measurements. The pore volumes measured for the two samples are shown in Fig. 5 as a function of pore diameter. It is clearly shown that the air-dried sample has few macropores, while the SCD sample has an extremely large pore volume of 9.8 $ml\,g^{-1}$, the most part of which comes from the pores ranging from 5–0.5 μm in diameter. The total pore volumes measured by the nitrogen adsorption study and the mercury porosimetry are summarized in Table II. It is interesting to note that the total mercury intrusion volume for the air-dried sample is only 1% of that for the SCD sample.

3.5. Scanning electron microscopy

Fig. 6 shows SEM photographs of the two dried samples. It is clearly shown that the SCD sample has a well developed card-house structure, and macropores are constructed by thin silicate sheet walls. From the photograph, it is also seen that most of the pores are approximately of 3–0.3 μm in diameter, in accordance with the data given by the above mercury porosimetry. In contrast to the SCD sample, in the air-dried sample the silicate layers are stacked on each other in a more regular manner, and only a small number of large pores are observed.

4. Discussion

As discussed elsewhere [8, 9], in the SiO_2–TiO_2 sol-pillared clays, the sol particles are intercalated and packed in multilayers between the silicate layers, so as to give a greater increase in the basal spacing. As a result, pores much smaller than the increment of the

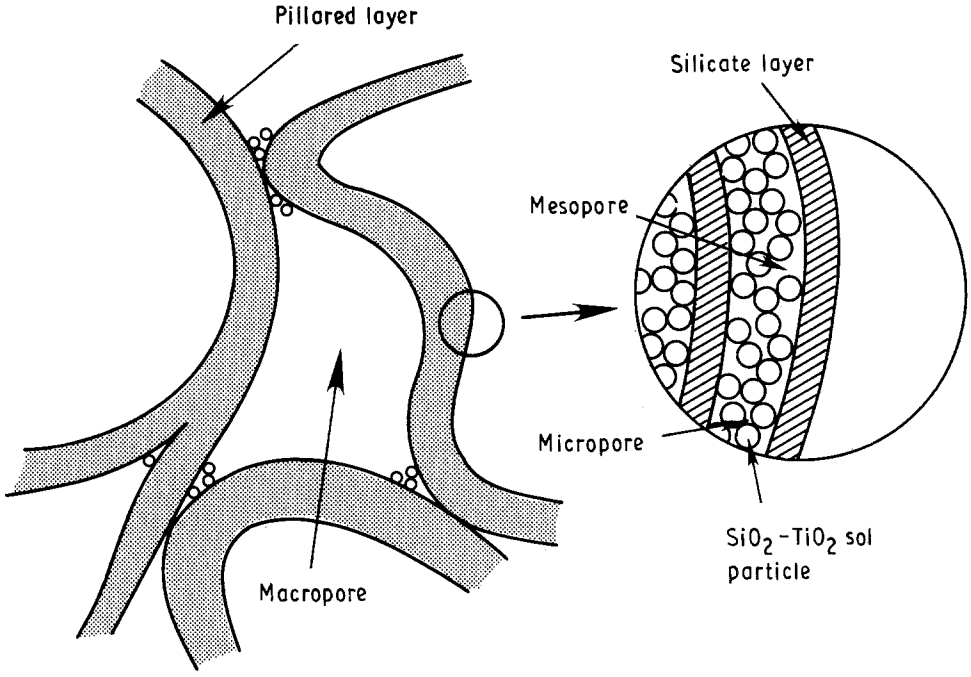

Figure 7 Schematic structural model of the pillared clay, supercritically dried sample.

basal spacing are formed in the spaces surrounded by the small, packed sol particles and the silicate layers of the clay. The pores measured by the nitrogen adsorption study are mainly attributed to such pores between the silicate layers. The formation of those pores, especially micropores, would not be much influenced by the drying method, as seen from the pore-size distribution curves in Fig. 4.

The macropores which were measured by mercury intrusion had been filled with water before drying. The macropores would disappear in a conventional evaporative drying procedure, because the strong interfacial forces between the swelled silicate layers lead to collapse of the pores on evaporation of the water. In the supercritical drying procedure, however, the water occupying the macropores is replaced with alcohol and then with a supercritical CO_2 fluid. In this case, the formation of liquid–vapour interfaces is avoidable and the delicate card-house structure constructed by the pillared silicate layer can be preserved during drying. The pore-volume data given in Table II show that the macropores shrink even to 1% of the original volume on air drying. From a different point of view, it is interesting to note that the sol-pillared clay is in an extraordinarily swelled phase before drying.

A schematic structural model showing the dual-pore structure of the SCD sample is shown in Fig. 7. The micro- and mesopores are located in between the loosely packed sol particles in the interlayer space of the pillared layers. The macropores are included in the highly porous card-house structure developed by the connection of the pillared layers.

Acknowledgement

The authors (S. Y. and M. H.) acknowledge the support of this study by a Grant-in-Aid for Developmental Scientific Research from the Ministry of Education, Science and Culture.

References

1. B. K. G. THENG, "The Chemistry of Clay-Organic Reactions" (Adam Hilger, London, 1974).
2. G. W. BRINDLEY and R. E. SEMPELS, *Clays Clay Miner.* **12** (1977) 229.
3. A. SCHUTZ, W. E. E. STONE, G. PONCELET and J. J. FRIPIAT, *ibid.* **35** (1987) 251.
4. S. YAMANAKA and G. W. BRINDLEY, *ibid.* **27** (1979) 119.
5. S. YAMANAKA and M. HATTORI, *Hyomen*, **27** (1989) 290.
6. S. YAMANAKA and M. HATTORI, "Chemistry of microporous crystals", edited by T. Inui, S. Namba and T. Tatsumi (Kodansha/Elsevier, Tokyo, 1991) p. 89.
7. S. YAMANAKA, T. NISHIHARA, M. HATTORI and Y. SUZUKI, *Mater. Chem. Phys.* **17** (1987) 87.
8. S. YAMANAKA, F. OKUMURA and M. HATTORI, in Extended Abstract of the 1986 Annual Meeting of the Ceramic Society, Tokyo, Japan (1986) p. 133.
9. S. YAMANAKA, T. NISHIHARA and M. HATTORI, *Mater. Res. Soc. Symp. Proc.* **111** (1988) 283.
10. R. ROY, *Science* **238** (1987) 1664.
11. G. W. SCHERER, in "Ultrastructure Processing of Advanced Ceramics", edited by J. D. Mackenzie and D. R. Ulrich (Wiley, New York, 1988) p. 295.
12. D. W. MATSONARD and R. D. SMITH, *J. Amer. Ceram. Soc.* **72** (1989) 871.
13. P. H. TEWARI, A. J. HUNT and K. D. LOFFTUS, *Mater. Lett.* **3** (1985) 363.
14. K. TAKAHAMA, M. YOKOYAMA, S. HIRAO, S. YAMANAKA and M. HATTORI, *J. Ceram. Soc. Jpn* **99** (1991) 14.
15. E. P. BARRETT, L. G. JOYNER and P. P. HALENDA, *J. Amer. Chem. Soc.* **73** (1951) 373.

Received 10 December 1990
and accepted 1 May 1991